hTetro: A Tetris Inspired Shape Shifting Floor Cleaning Robot

Veerajagadheswar Prabakaran, Mohan Rajesh Elara, Thejus Pathmakumar,
Shunsuke Nansai

Abstract — This research work presents the development of a novel tetris inspired reconfigurable floor cleaning robot – hTetro, utilizing the hinged dissection theory of polyominoes. The developed robot platform is capable of transforming between any of the seven set of one-sided tetromino morphologies according to the perceived environment with an objective of maximizing the coverage area. Experiments were performed across two different settings to systematically compare the coverage area performance of the developed hTetro robot and a commercially available fixed morphology robot platform. Results indicate significantly higher coverage area performance in the case of hTetro due to its ability to assume optimal morphology in relation to navigating environment.

I. INTRODUCTION

Due to faster pace of life in most developed world, floor cleaning is often seen as a dull, dirty, time consuming and tedious chore, giving rise to the development of robotic products for handling the cleaning task. Such robotic products have given their vast potential by improving productivity in cleaning jobs in domestic and commercial settings and witnessed steep rise over the last two decades [1]. It is expected that the floor cleaning robots would enter more households in the near future. It is estimated that between 2015 and 2018, about 25.2 million robotic cleaning units would be sold worldwide [2]. A number of successful products such as iRoomba, Neato XV-11, Samsung Powerbot, Bobsweep bobi, Miele scout, Moneual RYDIS, and Infinuvo CleanMate exist in the marketplace. These robots are generally characterized by circular morphology capable of autonomously mapping its environment using on-board sensors and navigate around the defined floor space to clean the environment efficiently.

Numerous research literatures deal with different aspects of floor cleaning robots such as mechanism design, human robot greatly affect their performance in cleaning attributed to their ability to navigate around highly complex terrains in social settings. Gao et al. presents the design of a floor cleaning robot equipped with Swedish wheels that can be highly efficient in terms of locomotion when used in crowded places such as train stations and airports [3]. A novel mechanism for mobility and control associated to a cleaning robot is described in the work mentioned in [4]. The above mentioned article focuses the methods for climbing up, down and translational movement that are required for cleaning stairs in addition to the conventional floor cleaning tasks. In terms of robot autonomy, Yang and Luo proposed a novel neural network based approach that accommodates the path planning with obstacle avoidance of cleaning robots in nonstationary environment [5]. The above mentioned methodology uses the previous location of robot and dynamic activity landscape of neural networks for the autonomous generation of robot path. In the article mentioned in [6], Siop et al. discusses a triangular cell map representation for the navigation of the cleaning robot with a shorter path and increased flexibilitywith increased flexibility and shorter path than a rectangular cell map representation. This work also proposes a complete coverage navigation and methods for map construction that enables the cleaning robot to perform navigation on the entire workspace with rudimentary information regarding the environment.

By tackling the cleaning task that is very much central to human lives, floor cleaning robots have attracted a number of human robot interaction studies. Fink et al. investigated the usage and scope of adopting a vacuum cleaning robot in various households by performing ethnographic studies for a period of six months [7]. This research also studied the evolution of cleaning robot over time, people's perception of the cleaning robot, tracking daily routines, analyzing the usage patterns and social activities related to the robot. Sakamoto et al. presents a stroke gesture based computer screen interface for commanding the cleaning robots [8]. This user interface allows the robot control and floor cleaning behavior generation by delineating the behaviors and actions of the robot by analysing the view from ceiling cameras. With respect to the use of multi-robot systems, Luo and Yang discusses a co-operative sweeping strategy using multi robot system using bio-inspired neural networks [9]. The above mentioned work discusses the complete coverage path planning using multiple cleaning robots in random and unstructured work space. The work metioned in [10] discusses a methodology for complete coverage path planning with two indoor floor cleaning robots to establish a minimal

This work was supported in part by the SUTD-JTC Infrastructure Innovation Incubation Centre Grant No. IPJTC31200110.

Veerajagadheswar is with SUTD-JTC Infrastructure Innovation Incubation Centre, Singapore University of Technology and Design, Singapore (Email: prabakaran@sutd.edu.sg)

Rajesh is with Engineering Product Development Pillar, Singapore University of Technology and Design, Singapore (Email: rajeshelara@sutd.edu.sg)

Thejus is with SUTD-JTC Infrastructure Innovation Incubation Centre, Singapore University of Technology and Design, Singapore (Email: thejus08@gmail.com)

Shunsuke Nansai is with SUTD-JTC Infrastructure Innovation Incubation Centre, Singapore University of Technology and Design, Singapore (Email: nansai_shunsuke@sutd.edu.sg)

turning path, based on the shape and size of the cells that covers the complete working area. The proposed algorithm utilizes the cellular decomposition strategy to decimate the whole cleaning area into cells and does efficient covering over the cells based on distance among centroids of cells.

With the rise of floor cleaning robotic prototypes and products, there has been an increasing trend in associated research into benchmarking these systems. Rhim et al. reports a set of performance index for autonomous mobile cleaning robot [11]. From author's perspective, the autonomy in mobility, ability for the dust collection, and noise for operation are the key performance indices for cleaning robots for the most real world applications. Wong et al. proposes two metrics for analysing the robot's cleaning performance and coverage efficiency and applied them to real time experiments [12]. The metrices for analyzing the performance are, measurement of covered area using computer vision technique and the distance covered by the cleaning robot.

Even though there exists numerous literature demonstrating the benefits of floor cleaning robots, the conventional floor cleaning robots suffer from a serious of performance issues that curtains their full potential. One major factor attributing to their performance loss is their fixed morphology design which highly constrains them when navigating such as room corners, narrow corridors between furniture and decorative artefacts. One viable approach to overcome this bottleneck is to design a next generation cleaning robot that is able to reconfigure its morphology in relation to the obstacles it encounters in space, thereby, maximizing cleaning performance.

The reconfigurable design has been studying and applied to robotics since the early 1980's. Numerous research works regarding the reconfigurable robotic systems have been proposed Since 1980. The development of reconfigurable designs and its practical implementation prove that, the re-configurability is a precious design strategy. Generally, the shape-shifting robots are classified into inter, intra and nested reconfigurable types [13]. An intra-reconfigurable robot can be treated as a conglomeration of sensors, actuators, mechanical parts, power, controller, etc., that acts as a single entity, capable of changing its internal morphology without requiring any external assembly or disassembly. The research works on the versatile amphibious robots capable of intra-reconfiguration between terrestrial and aquatic gait mechanisms [14], metamorphic robotic hands capable of intra-reconfigurable palm topologies [15], and reconfigurable walking mechanisms that produce a variety of locomotion gaits [16]. The second class of inter-reconfigurable robots consists of a congregation of modular homogenous or heterogeneous robots capable of forming a variety of morphologies through an ongoing assembly and disassembly process [17]. Relevant examples of inter-reconfigurable robots include CEBOT, PolyBot, Crystalline, M-TRAN, ATRON, Molecube, and CKBot. The third class of nested reconfigurable robots involve individual robots capable of intra-re-configurability while being able to assemble or disassemble with other homogeneous or heterogeneous robots (inter-re-configurability). Hinged-Tetro presented in [18] is an example of nested reconfigurable robot capable of both intra as well as inter-reconfigurable abilities. Even though, a vast literature on reconfigurable robotics are available, they are often limited to mechanism design with primitive pointers to potential applications. In addition, none of these work on reconfigurable robotics is targeted towards floor cleaning task, presenting numerous opportunities for research and development.

In this paper, we present a novel tetris inspired reconfigurable floor cleaning robot, hTetro based on the theory of hinged dissection of polyominoes. The developed robot platform is able to transform itself into any of the one-sided tetrominoes in relation to the obstacles encountered, thereby maximizing the cleaned area. The main challenges in designing a reconfigurable floor cleaning robot include the design of the shape-shifting mechanism, integration of vacuuming and sweeping features and the non-trivial process of implementing theoretical designs generated analytically into physical mechanisms. All these aspects are detailed in this paper, concluding with experimental results using the prototype hTetro robot that validates the proposed approach in comparison to a conventional fixed morphology robot. The reconfigurable hTetro robot herein presented is an initial design towards building a self-reconfigurable robot that is capable of autonomously changing its morphology in relation to the perceived obstacles in its environment and path plan with minimal set of reconfiguration steps.

Rest of this article is organized as follows: Section ''hTetro: Design Principle'' introduces the concept of polyominoes and hinged dissection. Section "hTetro: System Architecture" presents a discussion about the application of the theory of hinged dissection to realize a physical robot. This section also covers the core component modules of the developed robot namely the reconfigurable base, mobility unit, and the cleaning module. Sections "Experiments" and "Results and Analysis" presents elaborate details on the identified performance metrics, experimental method, set up, and analysis of the results with the prototype hTetro robot. Finally, the Section ''Conclusion'' concludes this study and discusses future work.

II. HTETRO: DESIGN PRINCIPLE

Polyominoes are two dimensional geometric structures formed by the edge wise connection of congruent squares. These Polyominoes form the central inspiration for the design of our hTetro robot and its reconfiguration strategies. Generally, a polyomino consisting of n squares is named as n-omino or n-polyomino [19]. Fig. 1 shows the formation of domino, triomino and tetromino with the edge

wise multiple combination of congruent squares. Polyominoes are popularly adopted in a number of entertainment puzzles since eighteenth century [20].

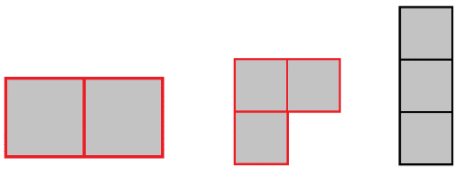

(a) One-sided Domino (b) One-sided Triomino

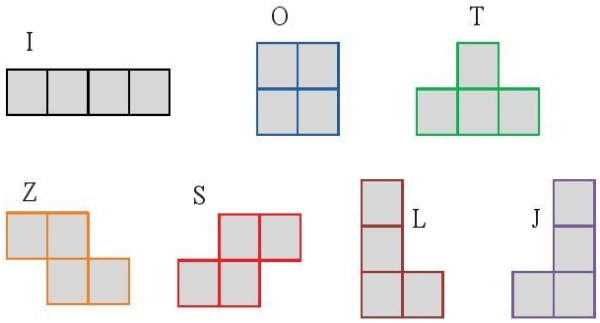

(c) One-sided Tetromino

Fig 1. Examples of Polyominoes.

Polyominoes can be classified as free Polyominoes, one-sided Polyominoes, and fixed Polyominoes based on their geometry and chirality. The free polyomino can be considered as a subset of the n-polyomino domain such that each individual elements exhibits chirality in terms of its spatial orientation. In the case of one-sided Polyominoes, the structure shows similarity in terms of its geometry, irrespective of right angled rotational transformations. Unlike the free polyominoes, the one-sided polyominoes does not shows chirality. Hence, the mirror image of the structure of each one-sided polyomino can be treated as another distinct element that belongs to the same subset. The fixed - polyominoes can be treated as another subset of the polyomino domain, such that each element (lattice animals) are distinct in terms of its rotational and flip transformations. Based on work presented in [21], single one sided, single free and two fixed dominoes form the domino group among the polyominoes. Similarly, two free, two one-sided, and six fixed triominoes (3-ominoes) forms the triomino group. It is also documented in [21] that for a group of tetrominoes, there exists five free, seven one-sided, and nineteen fixed tetrominoes. Since, the tetromino accommodates a large number of polymorphs, we adopted the geometrical structure of tetromino as the morphology for our self-reconfigurable cleaning robot. Our hTetro platform is capable of reconfiguring its morphology into any of the seven one-sided tetrominoes in response to perceived environment with the objective of achieving optimal coverage area and thereby cleaning performance. The strategy adopted in our work is analogous to the gap filling approach in common Tetris games. The fig. 1(c) illustrates the seven free tetromino structures that has been adopted for the dynamic morphology generation of hTetro robot.

The main challenge in the designing the hTetro robot is the placement of hinged dissection points that enables the shape shifting from one configuration to another. A hinged dissection is a geometric methodology that decimates a planar structure to finite number of pieces that are connected by “hinged” points in such a way that, a new shape can be created by rearranging the decimated pieces, without breaking the chain structure formed by the hinged points [22]. Fig. 2 illustrates the hinged dissection approach. Several works have been reported that deals with the concept of hinged dissection since 1984. For instance, hinged dissection has been used to transform an equilateral triangle into a polygon [23]. Another significant work is presented in [24] that demonstrates the usage of 3D hinged dissection for polypolyhedra involving connected 3D solids formed by merging several rigid copies of the same polyhedron along identical faces. In [25], a hinged dissection based approach to pattern generation is presented. Patterns are made in a way that when they are swung from one shape of the dissection to another, the patterns are also changed along with the shapes.

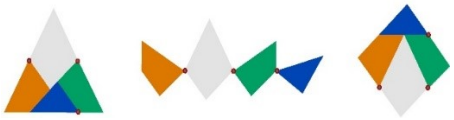

Fig 2. Example of Hinged Dissection

Current literature that deals with hinged dissection are generally confined to solving typical dissection problem in planar and spatial geometry. An innovative application of the hinged dissection has been dealt with in our previous work, where we developed a nested reconfigurable robot module called hinged-Tetro, and proved that LLR or LLL hinged dissection can be used to achieve the seven possible one-sided tetrominoes [18]. For the hTetro robot presented in this paper, we adopted the LLR hinged dissection shown in Table 1 to realize shape shifting capabilities.

TABLE I. Hinged Dissection of Tetromino in LLR Configuration

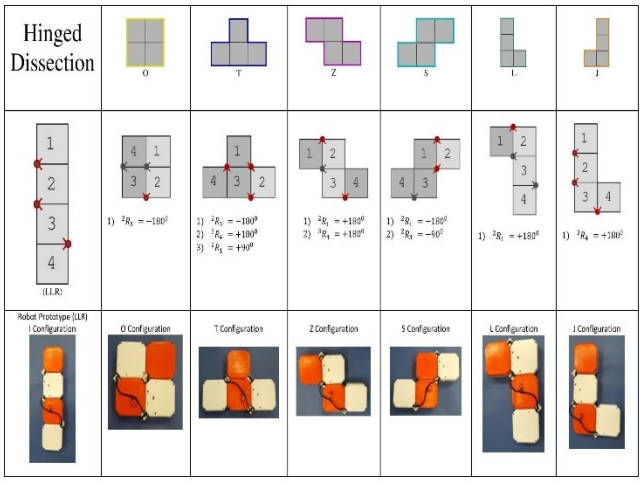

III. HTETRO: SYSTEM ARCHITECTURE

The design of our hTetro robot consists of four square blocks connected by a hinged dissection with each block responsible for a specific function. For instance, the first block executes the mobility function of the robot, the second block houses the control and power electronics modules, and the third and fourth blocks executes the cleaning function. Fig. 3(a) shows the CAD diagram of our hTetro robot in LLR hinged morphology.

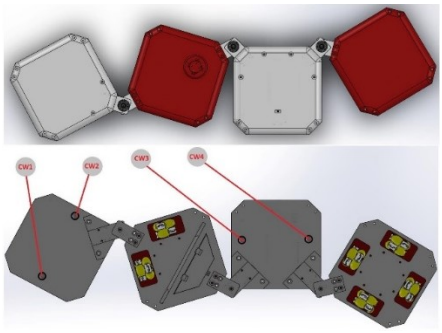

(a) Top view and Bottom view (block-4 to block-1)

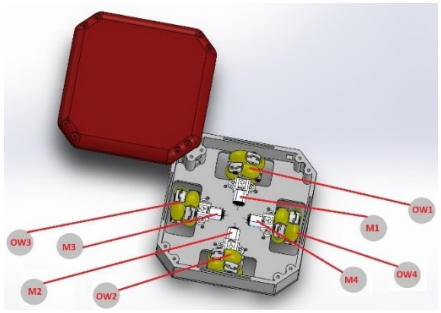

(b) Block-1

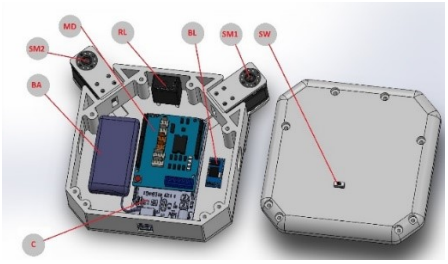

(c) Block-2

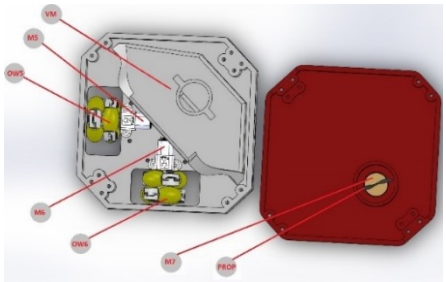

(d) Block-3

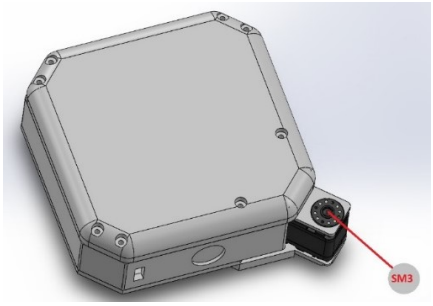

(e) Block-4

Fig 3. Robot's CAD and component used in each block

A. Mechanical Design

The enclosure of the robot has four square blocks connected by three active hinges. Each block has a dimension of 140 mm length, 140 mm width, and 55 mm height. The edges of each square block is chamfered to avoid the edge to edge collision during the reconfiguration process. The walls of the robot enclosure have a thickness of 4 mm. The enclosure is fabricated with hexagonal hollow spaces embedded like a honeycomb pattern to optimize the model in terms of minimum weight, maximum tensile strength and crack resistance. The enclosure and all the peripheral devices possesses a net weight of 4Kg. The robot transformation between any of the seven one-sided tetrominoes is realized through controlled actuation of the three active hinges. Fig. 3 illustrates the mechanical design of hTetro.

Mobility and transformation of the robot is attained using a set of nine motors. For robot's locomotion, six Pololu DC geared motors, with a working voltage of 7.4v has been used. The motors M1 to M4 are placed in the block 1 Fig. 3(b), acts as a main mobile unit for the robot. Motors M5 & M6 are placed in block-3 Fig. 3(d), aids in realizing stable locomotion. In 'I', 'S', and 'J' configurations, the motors M1, M2 & M5 are used for the forward and reverse motions and M3, M4 & M6 are used in left and right movement. In 'O', 'T', 'Z' and 'L' configurations, the motors acts vice versa. Omni-wheels (OW1-OW6) Fig. 3(a)(d) with a diameter of 48mm are driven by all the DC motors which makes the free movement possible in forward, reverse, left, and right directions. In addition to the Omni wheels, two caster wheels CW1-4 Fig. 3(a) were used to achieve maximum stability in block 2 and block 4 without affecting the ease of multi-directional locomotion. Three Herkulex DRS-0101-7V smart servos activates the hinges and controls the re-configurability. The smart servo motors can rotate to the maximum of 270 degrees and have an inbuilt encoder feedback system for precise control. The servos SM1 & SM2 attached with block 2 Fig. 3(c), acts as an anchor and drives both block 1 and block 3. SM3 that is placed in block 4 Fig. 3(d), drives block 4. Each servo has a stall torque of about 12 kg, which allows the motor to lock the positions of the blocks at the end of every transformation. When the robot starts moving, the blocks are locked automatically, so that the morphology of the robot is maintained throughout the robot's locomotion. Also, a high

rpm motor VM Fig. 3(d) is used for the robot's vacuuming function.

Locomotion and transformation of the robot are achieved through coordination between the actuators and the microcontroller. Arduino Atmega2560 16-Bit microcontroller is used which controls the locomotion, shape transformation and human robot interaction. The microcontroller is located in the second block of our robot Fig. 3(c). The microcontroller is programmed to carry out 3 major functions: (1) to generate control signals to motor driver unit MD that controls the (M1-M6) motors speed, (2) control signal generation for the servo motors (SM1-SM3) that realizes reconfiguration and receive feedback from it, and (3) receiving user commands from the remote smart phone device. The whole circuit is powered using a LIPO battery BA with 7.4v and 900mAh capacity. A toggle switch (SW) is connected in the main power supply branch, that enables the convenient making and breaking of the circuit. The detailed system architecture of electrical connections is shown in the Fig. 4. For each of the six motors, the speed and time period for the motor's rotations are defined by pulse-width modulation (PWM) signals from the microcontroller. The motor driver used here has four channels, to control four motors. Since, the robot has been deployed with six motors, a relay switch RL has been used to switch between the motors for different configuration. In every transformation the microcontroller gives a serial command (trough RX1 TX1 pin) to the SM1-3, and at the end of transformation the controller will receive the feedback from the motor's position from SM1-3 to cross check its position. Controller receives the wireless commands from (through RX0 TX0 pins) the remote user to perform the task for which a HC-06 (5v) Bluetooth device BL is used.

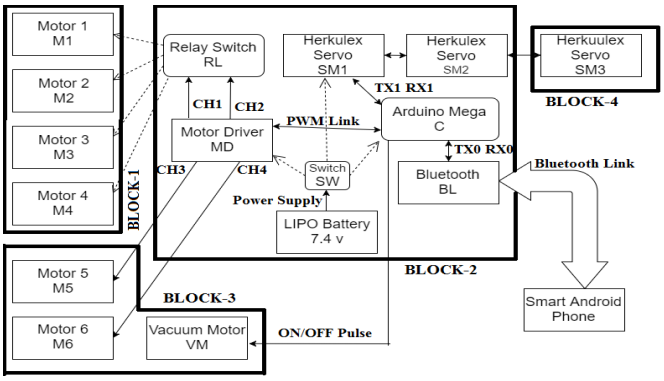

Fig 4. System Architecture of our robot.

B. *Software Design*

The default morphology for hTetro is set to be 'O' configuration shown in Fig. 7(b). For the experiments presented in this paper, the reconfigurations between the seven states were achieved upon receiving manual commands using an android smart phone application. Specifically, the user can choose most appropriate morphology based on the navigating environment in order to achieve maximum coverage. In our next prototype, we intend to make this process completely autonomous without human intervention. A software application for the user interface, as shown in Fig. 5 is developed for easy and efficient control. The developed application is installed in an android smart phone (2GHz octa-core Qualcomm Snapdragon 625 processor). The robot will perform the locomotion and shape reconfiguration according to the command sent from the application. Stop icon is used to terminate the robot's current action. To perform a 360° rotation clock wise or counter clock wise, bracket '(' ')' icons were used. Von & Voff is used to turn on and off the vacuuming function.

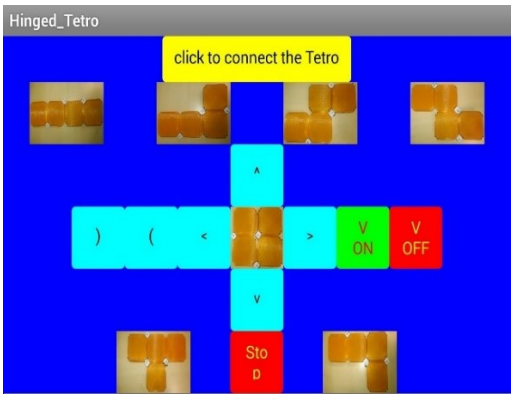

Fig 5. Graphical User Interface

IV. EXPERIMENTS

Two sets of experiments were conducted to evaluate and compare the performance of our robot, hTetro over a commercially available fixed morphology robot. The first set of experiments involved cleaning of a predefined area with a single furniture. We repeated the experiments across ten different types of furniture with five runs of trials for each furniture type. The average percentage coverage area across each of the ten experimental cases were computed for both hTetro and the commercial robot platform to compare their respective performances. Fig. 6 illustrates the ten furniture types involved in the first set of experiments. Each chair was ranked on a score of 1-10 on the basis of number of legs and their leg distance, due to the fact that the chair with more legs occupy large space and increase the complexity for cleaning task. During the second set of experiments, our hTetro's performance was compared over a fixed morphology robot in an office-like environment. Within the same experimental setting, the coverage area performance of both considered robots were computed across varying degree of obstacle density. To standardize the comparison, the commercial robot was reverse engineered to be manually controlled using an android smart phone application as with the case of hTtero. The fixed morphology robot used in the experiment is shown in Fig. 7(a). The experimental testbed consists of predefined floor area to be cleaned, support frames, image acquisition device, and an image processing algorithm that computes the coverage area automatically by tracking the robot within the operating space.

Fig 6. Chair types used in the experiment

Specification of fixed morphology robot

Fixed Morphology Robot	JNC Mini IQ Robot
Size of the Robot	28(diameter)X7.5(height) cm

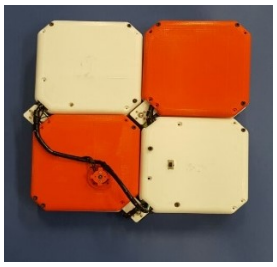

(a) (b)

Fig 7. Fixed morphology robot used for the experiment (a), default 'O' configuration of hTetro (b).

A. *Predefined Floor Area:*

The predefined floor area considered in this paper is a rectangular polished laboratory floor whose boundaries were defined by extendable metal frames. The surface area of the cleaning space can be varied by reconfiguring the arrangement of the extendable metal frames. For the first set of experiments, an area of 93x168 cm^2 and for second set of experiments an area of 200x168 cm^2 was used. The camera was placed perpendicular to the cleaning surface with fixed focal length. The altitude for fixing the camera was selected in such a way that, the whole cleaning area is covered in camera's field of view. We also ensured the movement of the robot will not get eclipsed by any of the obstacles. For instance, the seats of the chairs were removed, so that the image algorithm can track the robot's movement under the chair Fig. 8.

B. *Support Frame:*

Using T-slot aluminium extrusion profile, a parallelepiped structure was built to provide a vibration immune support for the camera mount over the cleaning space Fig. 9. The support frame has a dimension of 2000mm length, 2000mm breadth and 2500mm height. The camera was fixed exactly at the midpoint of the upper face of the supporting frame.

Fig 8. Experimental setup 1, after removing the chair's seat

Fig 9. Complete experimental setup

C. *Image Acquisition Device:*

The image acquisition device used was a digital HD camcorder with 2.07 Megapixel resolution connected to a computer. The camera has refresh rate of 24fps. The focal length of camera was fixed to 6.1 to 61mm and the auto focus functionality was disabled to ensure the fixed focal length. The videos of each experimental trials were recorded, and the raw recorded video files were converted to mp4 file format using a computer application Cyber Link Power Director. The mp4 files obtained after pre-processing format conversion was considered as the input for the image processing.

D. *Image Processing Algorithm:*

The image processing algorithm automatically computes the total area coverage performance of the robot under test by continuously tracking the area covered by that robot. The first step in the processing part is to save the first frame as a reference image for the track map generation. The second step in image processing algorithm is to detect the deployed robot and its position in each and every frame. The third step is to track map generation by plotting the identified position of the robot on the reference image. The coverage area performance is then calculated from the overlapped robot positions in the reference image. The implementation of this algorithm was completely done in MATLAB (R2015a). Since, the commercial cleaning robot used possesses a circular geometry, we used hough transformation based circle detection to determine the position of the geometric centre of the robot. Once the robot's centre is identified, a green coloured circle with same radius has been replicated on the reference image corresponding to the centre coordinates to generate the tracking map. Since, hTetro has a dynamic morphology, we used a colour based blob detection and tracking approach where the hTetro platform is detected by its four red blobs in each video frames. Using the detected blobs, the hTetro's area is identified and green squares are plotted on the reference image over the complete video sequence. After generating the tracking map on the reference image, the percentage of coverage area performance is calculated using Equation (1) for first set of experiments and Equation (2) for second set of experiments. In the equations (1) and (2), the

pixel area of the robot under test is computed by identifying the green coloured pixels on the track map on the reference image.

$$\%Coverage\ Area = \frac{\text{Pixels area of the robot}}{\text{Total pixels area of the testing field}} \times 100 \quad (1)$$

$$\%\ Coverage\ Area = \frac{\text{Pixel area of the robot}}{\text{Total pixel area of the testing field} - \text{Total pixel area of the obtacles}} \times 100 \quad (2)$$

V. RESULTS AND ANALYSIS

The performance of our hTetro robot was compared with a commercial cleaning robot across two different scenarios. The recording was started after the robot's position and the orientation was defined. Fig. 10 illustrates the tracking map on the reference image for both the robots under test. The area covered by the robots are represented by the green shades in the Fig. 10 based on the adopted image processing algorithm. We calculated the coverage area for both the robots under test using Equation 1 and 2. Fig. 11 shows the average percentage coverage area for both the robots in the first set of experiments involving five runs for each ranked furniture set.

Overall, the hTetro robot showed significantly better coverage area performance compared to the commercial fixed morphology robot considered. Interestingly, when the robots were tested with furniture ranking between 8-10, (i.e the chairs with multiple legs) the fixed morphology robot was not even able to access 50% of the defined area as shown in the Fig. 10. For the same test cases involving furniture ranking between 8-10, hTetro was able to achieve coverage area of over 80%. The average coverage area for hTetro over all the first set of experimental cases was found to be 94% while that for commercial fixed morphology robot was only 68%.

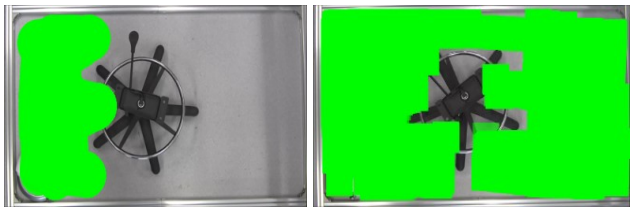

(a) (b)

Fig 10. Resulting tracking map on reference image for fixed morphology robot (a) and hTetro (b) around the furniture ranked 10.

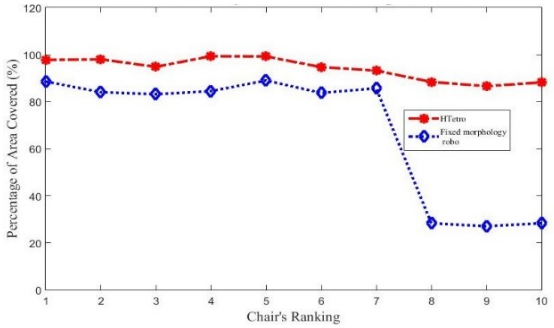

Fig 11. percentage of covered area by both the robots for first set of experiments

For the second set of experiments, the size of the testbed was extended by increasing the boundary. The camera lens was adjusted accordingly to capture the entire test site. The scenario was created to represent an office atmosphere with 6 pre-defined obstacles. The setup is shown in the Fig. 12.

(a) (b)

Fig 12. Testbed setup for second set of experiment, before (a), and after removing top surface of the furniture (b).

The obstacle density was calculated from the ratio of the pixels associated with the obstacles to the total pixels corresponding to the testing field. The tracking map generated on reference image for both robots captured during the second set of experiments involving 1 predefined obstacles with an obstacle density of 6% are shown in Fig. 13 (a) and (b). In this experiment the percentage of area covered was calculated for the accessible area within the testbed. For instance, the area covered by a dustbin, chamber, fan, and desk were subtracted from the total area to find the accessible area. Fig. 13 (c) and (d) shows the area covered by the robots upon increasing the obstacle density to 66% within the same testbed. Results clearly indicate significantly higher drop in performance for the commercial fixed morphology robot compared to our hTetro. Fig. 14 shows the average percentage coverage area for both the robots in the second set of experiments involving five runs for each obstacle density set. Again, hTetro achieved significantly higher coverage area as compared to the commercial robot considered.

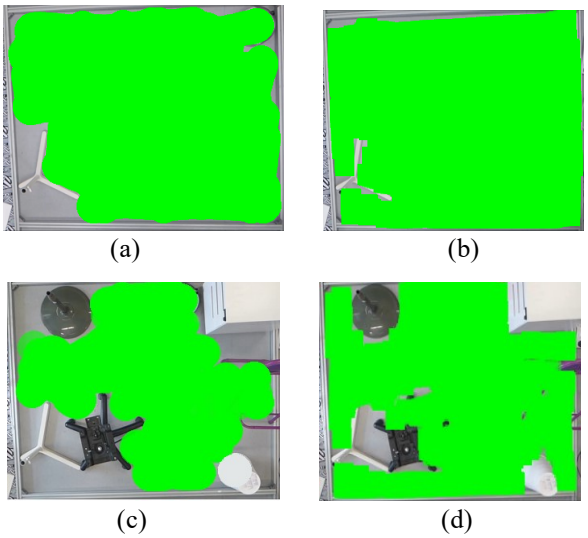

(a) (b)

(c) (d)

Figure 13. Resulting tracking map on reference image for fixed morphology robot (a & c) and hTetro (b & d), under increasing obstacle density

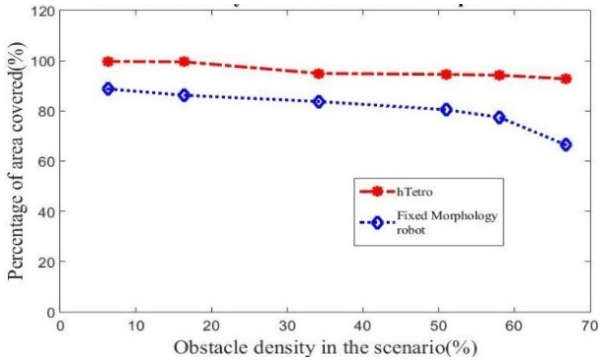

Figure 14. Percentage of area covered by both the robtos for second set of experiments

It was observed that the shape shifting mechanisms of hTetro enabled the robot to navigate through narrow tight spaces and corners within the testbed thereby nearly maintaining the coverage area performance even with increasing ranges of obstacle density tested. The average coverage area for hTetro over all the second set of experimental cases was found to be 95% while that for commercial fixed morphology robot was only 81%.

VI. CONCLUSION

In this paper, we presented a novel reconfigurable tetris inspired floor cleaning robot, hTetro that was developed using hinged dissection of polyominoes as basis. We validated the ability of the robot to transform between any of the seven one-sided tetrominoes morphologies in order to maximize the floor coverage area. Experiments were performed across two different settings to systematically compare the coverage area performance of the developed hTetro robot and a commercially available fixed morphology robot platform. Both the set of experiments performed indicate significant performance advantage in terms of floor coverage area for hTetro due to its ability to assume optimal morphology in relation to navigating environment. Future research will focus on: (1) development of a simulator to evalute tradeoffs between optimal configurations, path planning and coverage performance; (2) integration of cleaning modules in all the four blocks; (3) exhaustive experiments in highly diverse and complex environments to quantify the role of each of the seven configurations of hTetro in relation to the operating environment; and (4) development of additional features to improve power management issues and auto docking modes.

REFERENCES

[1] "IFR Robotics." Service robot Statics. 2016. Ifr.org. 1 Sep. 2016<http://www.ifr.org/service-robots/statistics/>.

[2] "Robotics." Encyclopedia of Management. 2009. Encyclopedia.com. 1 Sep. 2016<http://www.encyclopedia.com>.

[3] Gao, Xueshan, et al. "A floor cleaning robot using Swedish wheels."Robotics and Biomimetics, 2007. ROBIO 2007. IEEE International Conference on. IEEE, 2007.

[4] Kakudou, Takahisa, Keigo Watanabe, and Isaku Nagai. "Study on mobile mechanism for a stair cleaning robot-Design of translational locomotion mechanism." Control, Automation and Systems (ICCAS), 2011 11th International Conference on. IEEE, 2011.

[5] Yang, Simon X., and Chaomin Luo. "A neural network approach to complete coverage path planning." IEEE Transactions on Systems, Man, and Cybernetics, Part B (Cybernetics) 34.1 (2004): 718-724.

[6] Oh, Joon Seop, et al. "Complete coverage navigation of cleaning robots using triangular-cell-based map." IEEE Transactions on Industrial Electronics 51.3 (2004): 718-726.

[7] Fink, Julia, et al. "Living with a vacuum cleaning robot." International Journal of Social Robotics 5.3 (2013): 389-408.

[8] Sakamoto, Daisuke, et al. "Sketch and run: a stroke-based interface for home robots." Proceedings of the SIGCHI Conference on Human Factors in Computing Systems. ACM, 2009.

[9] Luo, Chaomin, and Simon X. Yang. "A real-time cooperative sweeping strategy for multiple cleaning robots." Intelligent Control, 2002. Proceedings of the 2002 IEEE International Symposium on. IEEE, 2002.

[10] Janchiv, Adiyabaatar, et al. "Complete coverage path planning for multi-robots based on." Control, Automation and Systems (ICCAS), 2011 11th International Conference on. IEEE, 2011.

[11] Rhim, Sungsoo, et al. "Performance evaluation criteria for autonomous cleaning robots." 2007 International Symposium on Computational Intelligence in Robotics and Automation. IEEE, 2007.

[12] Wong, Sylvia C., et al. "Performance metrics for robot coverage tasks."Proceedings of Australasian Conference on Robotics and Automation. Vol. 27. 2002.

[13] Tan, Ning, et al. "Nested reconfigurable robots: theory, design, and realization." International Journal of Advanced Robotic Systems 12 (2015).

[14] Y. Sun and S. Ma. epaddle mechanism: Towards the development of a versatile amphibious locomotion mechanism. In IEEE/RSJ International Conference on Intelligent Robots and Systems, pages 5035–5040, 2011.

[15] G. Wei, J. Dai, S. Wang, and H. Luo. Kinematic analysis and prototype of a metamorphic anthropomorphic hand with a reconfigurable palm. International Journal of Humanoid Robotics, 08(03):459–479, 2011.

[16] S. Nansai, N. Rojas, R.E. Mohan, and R. Sosa. Exploration of adaptive gait patterns with a reconfigurable linkage mechanism. In IEEE/RSJ International Conference on Intelligent Robots and Systems, pages 4661–4668, 2013.

[17] Hongxing Wei, Ning Li, Yong Tao, Youdong Chen, and Jindong Tan. Docking system design and self-assembly control of distributed swarm flying robots. International Journal of Advanced Robotic Systems, 9(186), 2012.

[18] Kee, Vincent, et al. "Hinged-Tetro: A self-reconfigurable module for nested reconfiguration." 2014 IEEE/ASME International Conference on Advanced Intelligent Mechatronics. IEEE, 2014.

[19] S. Golomb, "Checkerboards and polyominoes," The American Mathematical Monthly, vol. 61, no. 10, 1954.

[20] S. Coffin and J. Slocum, "What's new in polyomino puzzles and their design," in Mathematical Properties of Sequences and Other Combinatorial Structures, ser. The Springer International Series in Engineering and Computer Science, J.-S. No, H.-Y. Song, T. Helleseth, and P. Kumar, Eds. Springer US, 2003, vol. 726, pp. 113–119.

[21] D. Klarner, "Polyominoes," in Handbook of Discrete and Computational Geometry, J. Goodman and J. O'Rourke, Eds. CRC Press, 1997, ch. 12.

[22] G. Frederickson, Hinged Dissections: Swinging and Twisting. Cambridge University Press, 2002.

[23] E. Demaine, M. Demaine, D. Eppstein, G. Frederickson, and E. Friedman, "Hinged dissection of polyominoes and polyforms," Computational Geometry, vol. 31, no. 3, pp. 237 – 262, 2005.

[24] Erik D. Demaine1, Martin L. Demaine1, Jeffrey F. Lindy, and Diane L. Souvaine3, "Hinged dissection of polypolyhedra," Volume 3608 pp 205-217

[25] Sarhangi, Reza. "Making patterns on the surfaces of swing-hinged dissections." Bridges Leeuwarden Proceedings (2008): 251-258.